Available online at www.sciencedirect.com
ScienceDirect
Ceramics International 36 (2010) 1083–1090
CERAMICS INTERNATIONAL
www.elsevier.com/locate/ceramint

On the shear strength of laser brazed SiC–steel joints: Effects of braze metal fillers and surface patterning

I. Südmeyer *, T. Hettesheimer, M. Rohde

Karlsruhe Institute of Technology, Institute for Materials Research I, Hermann-von-Helmholtz-Platz 1, 76344 Eggenstein, Germany

Received 11 June 2009; received in revised form 22 October 2009; accepted 23 November 2009
Available online 4 January 2010

Abstract

Within the development of a laser brazing process for joining non-oxide ceramics (SiC) to steel, we examined the effect of different braze filler metals on the shear strength of the joint. Specific surface patterns were applied on the surface of the ceramic in order to study changes of the joint strength by an additional mechanical anchoring at the ceramic–braze metal interface.

The study compared a commercial AgCuTi brazing foil with SnAgTi-alloys, which contained various Sn/Ag fractions, with regard to their implementation in the laser process, which is characterized by localized heat input and short processing times in contrast to conventional furnace brazing. The microscopic investigations on laser brazed cross-sections indicated, that the application of the AgCuTi foil developed porous metal–ceramic interfaces with a poor mechanical stability and a high failure rate. The application of SnAgTi-alloys within the laser process resulted in an interface, which is free of pores. The characteristic fracture shear stress increased with increasing Sn fraction up to $\tau_0 = 20$ MPa and a Weibull modulus of $m = 4.9$ for the 50Sn48Ag2Ti alloy. A further enhancement of the shear strength could be achieved by generating specific patterns on the surface of the ceramic prior to the laser brazing process.

Keywords: Laser brazing; Laser structuring; Ceramic–steel joint

1. Introduction

The excellent properties of SiC like thermal stability, corrosion and wear resistance are of major interest for high performance engineering systems. In order to profit from the advantages of this ceramic, the integration into metallic structures for the manufacturing of complex shaped components becomes necessary. The choice of an appropriate joining technique is dependent on the combination of the materials to be joined, the thermal and mechanical loads on the joints within the application and the design of the component. Especially, for ceramic–metal-joints, that are thermally and mechanically stressed, brazing can be an adequate solution.

However, brazing of ceramics is associated with some particularities. One of these is the poor wettability of ceramics by conventional brazing alloys, which can be enhanced by adding active elements for ceramic surface activation, e.g. Ti or Zr [1–6]. The most frequently used active braze fillers are AgCuTi-alloys, which are utilized in furnace brazing processes under a controlled inert gas atmosphere or vacuum. For these process conditions the AgCuTi braze alloys have been exhibiting a good wetting and joining behaviour with oxide and non-oxide ceramics [1–4,7–9].

Another problem, which is associated with the joining of metals to ceramics, is the generation of residual stresses, which are caused by the dissimilar elastic and thermal properties of the two material groups, i.e. Youngs modulus and coefficient of thermal expansion. These give rise to reduction of the joint strength [5,6,10]. The residual stresses are also affected by the process conditions and the geometry [5,6,10,11]. They can be reduced by the addition of ductile and therefore stress reducing elements like Cu, either within the braze filler material or as an interlayer. Alternatively, an interlayer material possessing a coefficient of thermal expansion, which is similar to the ceramic, may minimize the compound stresses by feeding the high stresses from the ceramic to the metal joining partner [12–17]. Furthermore, particle reinforced braze fillers are known to increase the compound strength [18,19]. The influence of

* Corresponding author. Tel.: +49 07247 823390; fax: +49 07247 824567.
E-mail address: isabelle.suedmeyer@kit.edu (I. Südmeyer).

0272-8842/$36.00 © 2010 Published by Elsevier Ltd and Techna Group S.r.l.
doi:10.1016/j.ceramint.2009.12.010

Table 1
Material properties.

Material/Composition	PLS-SiC	Ag-Cu-Ti 70.5-26.5-3	Ag-Cu-In-Ti 59-27.2-12.5-1.25	Sn-Ag-Ti 30-68-2	Sn-Ag-Ti 40-58-2	Sn-Ag-Ti 50-48-2	Steel Matno. 1.1191
Trade name	EKasic-F	CB 4	Incusil-ABA	30Sn68Ag2Ti	40Sn58Ag2Ti	50Sn48Ag2Ti	C45E
Company	ESK Ceramics	Brazetec	Morgan Chem.	Research Centre Karlsruhe, IMF I* *Sn, Ag: Alfa Aesar GmbH, Germany, Ti: Fluka			
Average grain/particle size (μm)	1.9			Sn: 11 μm; Ag: 0.6–2 μm; Ti: 380 μm			
Density ρ (g/cm^3)	3.9	9.9	9.7	9.3	9.0	8.7	7.9
Strength σ (MPa)	350	230	338	-	-	-	620
Youngs Modulus E (GPa)	380	72	76	63	61	59	212
Coefficient of thermal expansion CTE (10^{-6}/K)	8.4	18.9	18.2	-	-	-	11.1
Brazing temperature T_{braze} (°C)		900–950	850–900	900–950			

surface roughness, textures and structured interlayer on the wetting and joining behaviour is also important for the strength of brazed ceramic–metal-joints [20–22].

The thermal process parameters, particularly the brazing temperature and the dwell time, influence the joint strength [23–26], since they control the intensity and duration of the reaction between the active element in the braze metal filler and the ceramic. Both should be set in order to achieve an optimized thickness of the reaction layer without the development of brittle reaction phases [23,25,26].

The influence factors described above and its consequences on metal–ceramic brazing have been mainly studied for the furnace brazing process, which is characterized by slow heating and cooling cycles while the whole component is placed in a nearly uniform temperature field. Therefore, the knowledge base for this type of process related to metal–ceramic brazing is relatively broad. In contrast to that the important features of a laser brazing process are options for rapid heating and cooling with a localized heat input by the laser beam, which is focused onto the joining zone.

Due to these differences in the characteristic scales in space and time for the laser and furnace brazing process, respectively, it can be expected that also specific properties of the metal–ceramic joint may differ at least as long as the kinetic aspects of the reaction, spreading and wetting of the braze metal on the ceramic surface is considered. Unfortunately, the data base for the laser based processes applied to metal–ceramic joining is very small. This may also be an obstacle for a transfer into industrial applications utilizing metal–ceramic components [27,28].

The objective of this study was to clarify possible differences in the joint strength and the failure mode using two different braze metal fillers applied in the laser brazing process for joining SiC to steel. Commercially available AgCuTi braze metals, which have been successfully tested within a previous study of laser brazing of Al_2O_3 to steel [29], were compared with SnAgTi type braze fillers, which proved to achieve a good wettability on SiC [30].

The work of Nicolas and Standing has proved the beneficial effects of ternary alloying elements with a low surface energy and low solubility of Ti, like Sn, on the wetting of ceramic surfaces. This regularity was shown for Cu–Sn–Ti alloys. A similar effect can be achieved for SnAgTi-alloys because Ag alike Cu exhibits a higher surface energy than Sn [1,31]. Also the Sn based braze metal was selected since the solidus temperature can be adjusted by varying the Sn content.

Additionally, the influence of different surface patterns applied to the surface of the SiC–ceramic on the joint strength was studied.

2. Materials and methods

2.1. Materials

For the joining studies a pressureless sintered SiC (Ekasic-F, Comp: ESK Ceramics) was selected. The steel was C45E (Matno. 1.1191). One commercial active brazing foil, an AgCuTi-alloy (B-70.5AgCuTi-800, CB4, BrazeTec) was applied. Furthermore, braze pellets with different SnAgTi-compositions (Sn- and Ag-powder: Alfa Aesar GmbH, Ti-powder: Sigma–Aldrich) were manufactured by mixing the base metal powders followed by a compaction step using axial pressing. The properties of the ceramic, brazes and steel, are listed in Table 1.

The geometry of the cylindrical samples used for laser joining is shown in Fig. 1. The cylinders measured an outer diameter of 16 mm. The ceramic parts had a height of 4 mm and the metal carrier was 16 mm high. The metal probes received a centre hole of 12 mm in depth and 12 mm in diameter, that allowed a heating close to the joining zone (Fig. 1). The metal and the ceramic joining faces were ground with 600 graining.

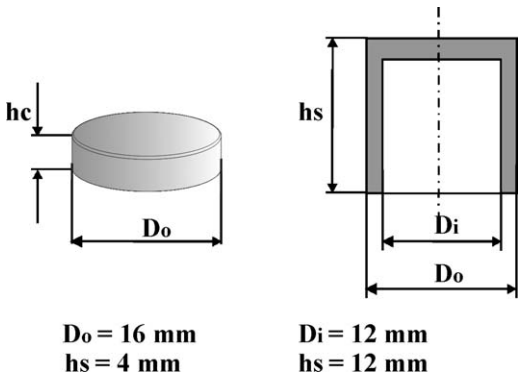

Fig. 1. Geometry of the ceramic (left) and the metal (right) joining component.

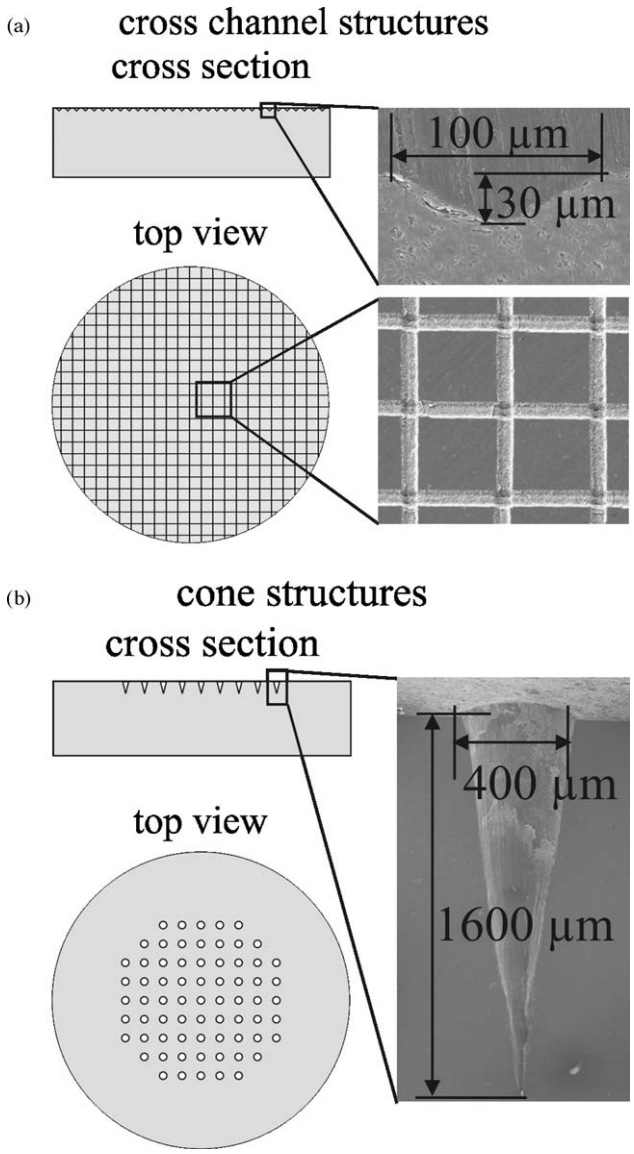

Fig. 2. Laser induced structures on the ceramic joining surfaces: (a) crossed channels and (b) cones.

Two different patterns were manufactured on selected ceramic surfaces (Fig. 2). These patterns were generated by a Nd:YAG laser operating at a wave length of 1064 nm using a direct writing process, which removes the material by laser ablation. One surface texture represented crossed channels ($w = 100$ mm, $h = 30$ μm) as shown in Fig. 2a, and the second series of ceramic pellets were patterned with an assembly of 71 cone shaped structures. Each of the single structure elements had a diameter of 400 μm and a depth of 1600 μm (Fig. 2b).

2.2. Process technology

Before the laser process the ceramic pellet and the steel base were mounted in a fixture, which is schematically shown in Fig. 3a. The brazing foil or pellet ($s = 200$ μm) was placed between the ceramic and the steel and a pressure of approximately $p = 2$ MPa was applied. The laser sided metal surface was sandblasted and carbon coated in order to prevent

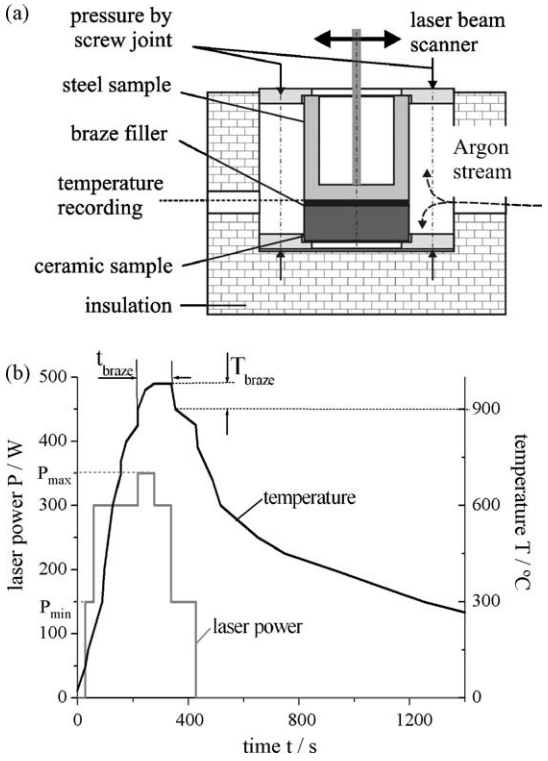

Fig. 3. Process of laser brazing: (a) arrangement for laser brazing of cylindrical samples and (b) laser power and probe temperature as a function of processing time for a SiC–50Sn48Ag2Ti–steel compound.

reflection and to improve the absorption. The warming up was also realized by the CO_2-laser scanning system ($\lambda = 10.6$ μm) with the beam path covering the inner diameter of the steel bar with a sequence of 12 horizontal lines under permanent rotation. This procedure ensured a homogenous warming of the composite. During brazing an argon stream of 300 Nl/h was directed onto the joining zone for avoiding oxidation of the active braze filler and the metal.

The laser power was increased stepwise until the brazing temperature was achieved. By a reduction of the laser power the brazing temperature was held for a maximum of 120 s. Afterwards the laser power was decreased gradually. The whole laser process lasted approximately 400 s. During brazing and cooling the temperature was measured in the joining zone by a pyrometer. The measured temperature as a function of time is shown in Fig. 3b. The corresponding laser power, which is applied to the steel base, is also given in the diagram.

2.3. Mechanical testing

The compound strength of the laser brazed samples was evaluated by shear loading, which is a common method for strength evaluation of brazed ceramic–steel joints [4,6,26,32,33]. The shear test configuration is shown schematically in Fig. 4. The steel base was clamped completely up to the steel–braze metal interface and the shear load was applied to the ceramic via a tempered plunger.

The gadget was positioned in a universal-testing machine (INSTRON), in which the force was applied at a velocity of

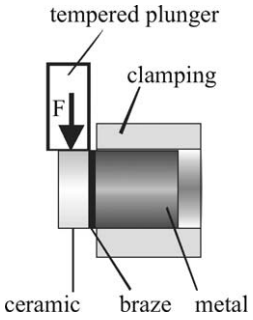

Fig. 4. Shear testing configuration of the brazed ceramic–steel joints.

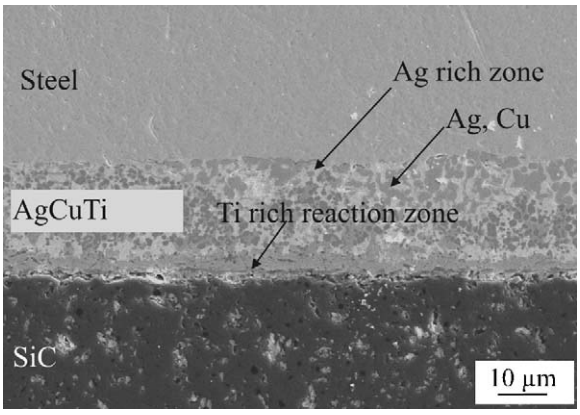

Fig. 5. SEM image of a laser brazed SiC–AgCuTi–steel compound. The element distribution was analyzed by EDX.

0.05 mm/s. Based on the measured fracture load F_B the fracture shear strength τ_B was determined according to Eq. (1):

$$\tau_B = \frac{F_B}{\pi \cdot R^2} \quad (1)$$

with the sample radius R.

A minimum of ten samples for each probe series was tested and the fracture strength values were interpreted according to the Weibull theory [34]. In that manner the characteristic fracture shear stress τ_0 at a fracture probability of 63.2% and the Weibull modulus m were specified as characteristic properties in the following.

3. Results and discussion

3.1. Compound analysis

The laser brazing experiments resulted in a poor wetting behaviour for SiC with the AgCuTi-filler. Either no wetting or a poor adhesion between the ceramic and braze metal was achieved with these brazing alloys. In Fig. 5, a cross-section of a SiC–steel compound brazed with AgCuTi is shown. Although a Ti-rich reaction zone has developed towards the ceramic interface, a non-continuous wetting with numerous pores characterizes the connection between braze and ceramic. The EDX-analysis of the reaction layer proved apart from Ti, fractions of Si, which diffused from the ceramic. In Table 2, the results of the EDX-analysis are listed for the reaction layers of all compounds.

The attempt of improving the bonding between SiC and the AgCuTi-fillers through surface modifications, which included several surface structuring methods, e.g. sandblasting as well as surface coatings of TiC and chemical surface modification by NiP-plating, failed. None of these pre-conditioning measures succeeded in an improved wetting and adhesion behaviour of the AgCuTi braze fillers with SiC.

In order to compare the AgCuTi-system with a second type of braze filler, which may be better adapted to the laser brazing process, the joining behaviour of SnAgTi type braze metal with varying compositions was studied. Due to its lower solidus temperature, which is determined by the Sn fraction, it can be expected, that also the wetting and spreading of the Sn based braze metal is better suited for the fast heating and cooling of the laser process. Moreover the low surface energy of Sn has a positive effect on the Ti activity as described above [1,30].

Preliminary tests exhibited a non-wetting behaviour for braze fillers with fractions of Sn lower than 25 wt.%. For that reason only braze fillers, that contained Sn fractions above 30 wt.%, were included in the present study, namely the compositions 30Sn68Ag2Ti, 40Sn58Ag2Ti and 50Sn48Ag2Ti.

The microscopic and EDX-analyses of the brazed compounds with differing SnAgTi-compositions resulted in very

Table 2
EDX-analyses of ceramic–braze interfaces for different brazing alloys.

		EDX-analyses						
		Elements						
		Ag	C	Cu	Si	Sn	Ti	Total
Braze filler	Interface	at.%						
AgCuTi	Ti rich	5.13	–	6.81	9.16	–	78.90	100
30Sn68Ag2Ti	Ti rich	0.56	62.22	–	0.65	0.90	35.67	100
	Ti free	2.18	45.28	–	3.73	48.81	–	100
40Sn58Ag2Ti	Ti rich	1.03	59.18	–	20.75	2.15	16.89	100
	Ti free	81.33	–	–	–	18.67	–	100
50Sn48Ag2Ti	Ti rich	1.07	11.77	–	3.20	67.72	16.24	100
	Ti free	47.30	36.86	–	–	15.84	–	100

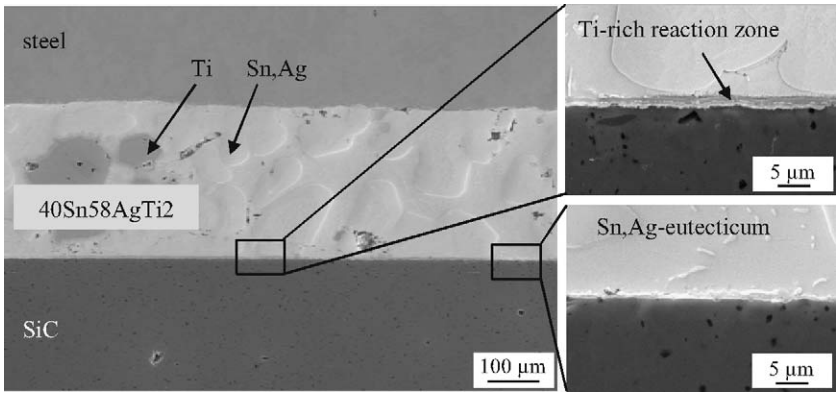

Fig. 6. SEM image of a laser brazed SiC–40Sn58Ag2Ti–steel compound.

similar cross-sections. Micrographs of SiC-steel joints, which were brazed with two different Sn/Ag-ratios, are shown in Figs. 6 and 7, respectively. In Fig. 6, a compound brazed with 40Sn58Ag2Ti is presented and Fig. 7 shows a SiC–50Sn48Ag2Ti–steel joint.

In both braze layers the dominant, light grey part is composed of a SnAg-eutecticum. Within these eutectic phases the dark grey areas were detected to be Ti particles. Two different, irregular distributed areas were recognized towards the braze–ceramic interface, which are marked in Figs. 6 and 7. In some sections thin Ti-rich reaction layers were formed without pores or failures. These reaction zones contained Sn from the braze filler as well as Si and C diffused from the ceramic (Table 2). The Ti fraction in these reaction layers ranged from 10 to 40 at.% without a recognizable dependence on the SnAg fraction.

In the second kind of section no dark grey reaction layer was visible, but a light grey area similar to the interface distant regions is recognized. The EDX-analysis of these areas showed SnAg-eutectica containing fractions of Si and C. Still very few seams were distinguishable in these Ti free interfaces. The composition of the ceramic–braze interface zones covered a wide variation but no characteristic composition (Table 2). In that manner the EDX-analysis did not give a reasonable explanation for the poor wetting of AgCuTi-filler. Also, no explicit differences of element contents or wetting between the various SnAgTi-fractions were found, which could be reference for one SnAgTi-fraction to be superior to another.

Experiments showed that the Ti-rich reaction layer could not forced to be more expanded by extra brazing time or a higher amount of Ti. This may be ascribed to the large average Ti particle size $d_a = 380$ μm in comparison to the much smaller Sn and Ag-powder particles (Sn: $d_a = 11$ μm and Ag: $d_a = 0.6$–2 μm). The mobility of the surface activating particles was reduced within the interfaces, so that the formation of a wider reaction zone was restricted.

3.2. Shear tests

The measured shear strength values of the joints, which were brazed with different SnAgTi-compositions, are plotted in a Weibull diagram shown in Fig. 8. At first sight one general tendency was visible: an increasing Sn fraction resulted in rising shear strength. Whereas the microscopic analysis exhibited no explicit differences in the wetting behaviour of the braze variations, the mechanical testing proved, that the joining behaviour was influenced by the Sn content. The characteristic shear strength τ_0 increased from $\tau_0 = 15.7$ MPa for 30Sn68Ag2Ti to $\tau_0 = 19.1$ MPa for 50Sn48Ag2Ti. Also the reliability of the joints was improved through a higher amount of Sn in the braze fillers. The compounds brazed with the lowest Sn fraction exhibited a Weibull modulus of only $m = 2.7$, in

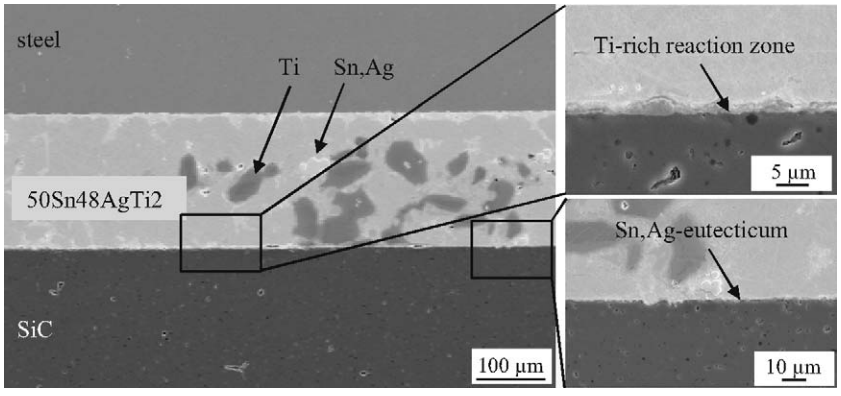

Fig. 7. SEM image of a laser brazed SiC–50Sn48Ag2Ti–steel compound.

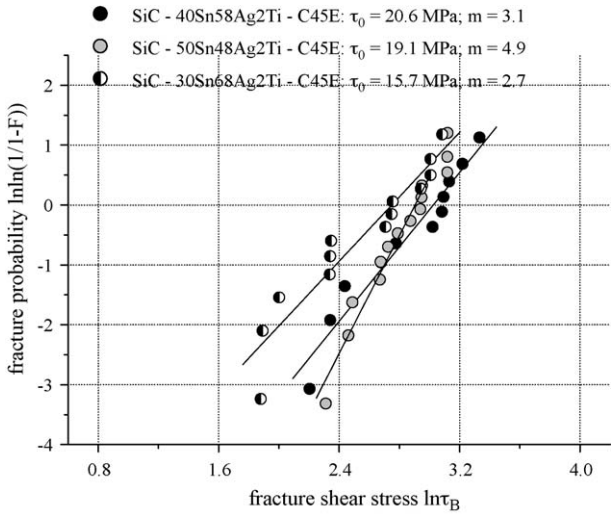

Fig. 8. Shear strength and corresponding fracture probability of compounds brazed with different SnAgTi-fractions.

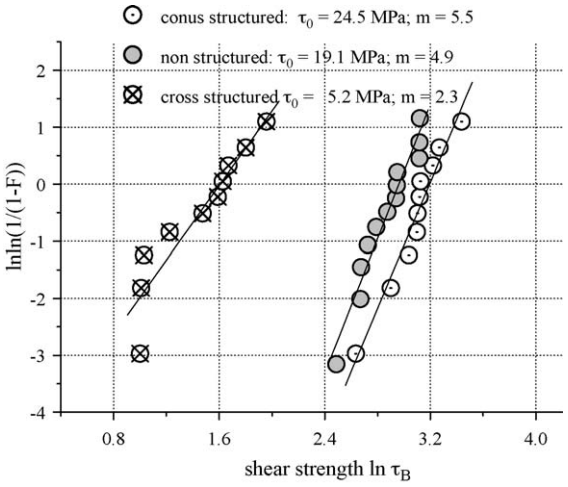

Fig. 10. Shear strength and corresponding fracture probability of SiC–50Sn48Ag2Ti–steel compounds brazed with non-structured and structured ceramic surfaces.

comparison to the 50Sn48Ag2Ti-joints, that accomplished a Weibull modulus of $m = 4.9$.

The fracture lines proceeded similarly for all SnAgTi-fractions along the ceramic–braze interfaces. As an example the metal and the ceramic part of a SiC–50Sn48Ag2Ti–steel joint are shown in Fig. 9. The active braze filler adhered well to the complete metal surface, but only to a small part of the ceramic surface after fracture. It was assumed that the poor Ti-rich reaction zone discussed above was responsible for the weak bond between ceramic and braze, so that the origin of fracture line were located at this interface with the poor adherence as the predominant reason for failure.

Since the SiC-steel joints brazed with 50Sn48Ag2Ti showed good characteristic shear strength values, the ceramic pellets with the surface patterns were also brazed with this SnAgTi-alloy. The results of the shear strength determination for the structured and non-structured SiC–50Sn48Ag2Ti–steel-joints are summarized in Fig. 10. In comparison to the non-structured ceramic–steel joints with a strength of $\tau_0 = 19.1$ MPa, a strong decrease of the shear strength for the crossed channel structures with a characteristic shear strength of $\tau_0 = 5.2$ MPa could be observed. An examination of the fracture surfaces (Fig. 11) exhibited a fracture along the ceramic–braze interfaces for all cross-channel structured ceramics.

However, the surface patterning with the cone shape structures significantly enhanced the shear strength up to $\tau = 24.5$ MPa. Inspection of the fracture surfaces indicated (Fig. 12), that the fused braze filled the cones only to a depth of

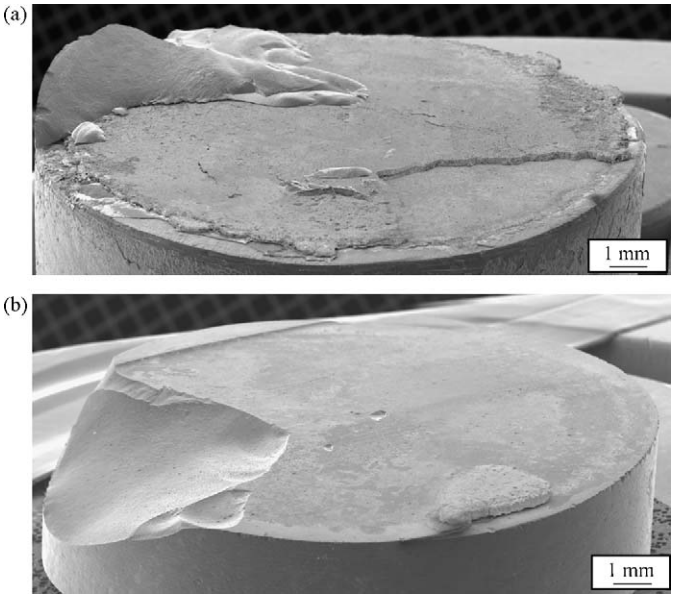

Fig. 9. SEM image (tilt angle $\alpha = 65°$) of a fracture surface of a non-structured ceramic–steel joint: fracture line runs through the ceramic and along the ceramic–braze interface (a) metal part and (b) ceramic part.

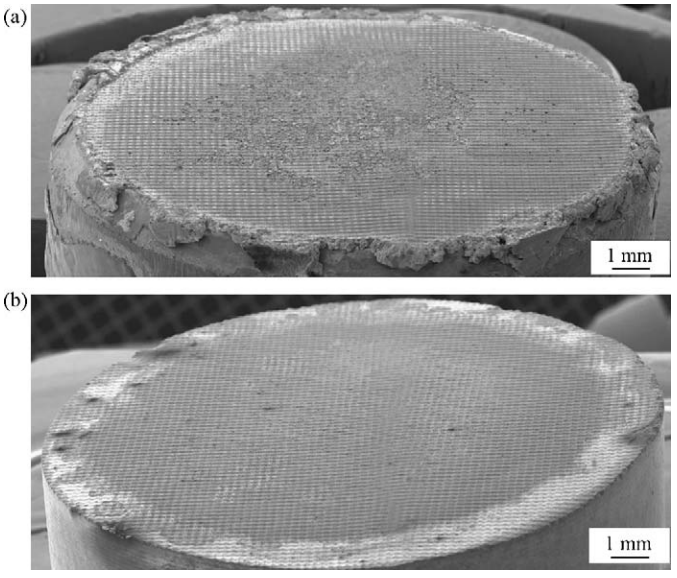

Fig. 11. SEM image (tilt angle $\alpha = 65°$) of a characteristic fracture surface of a channel structured ceramic–steel joint: fracture line runs along the ceramic–braze interface (a) metal part and (b) ceramic part.

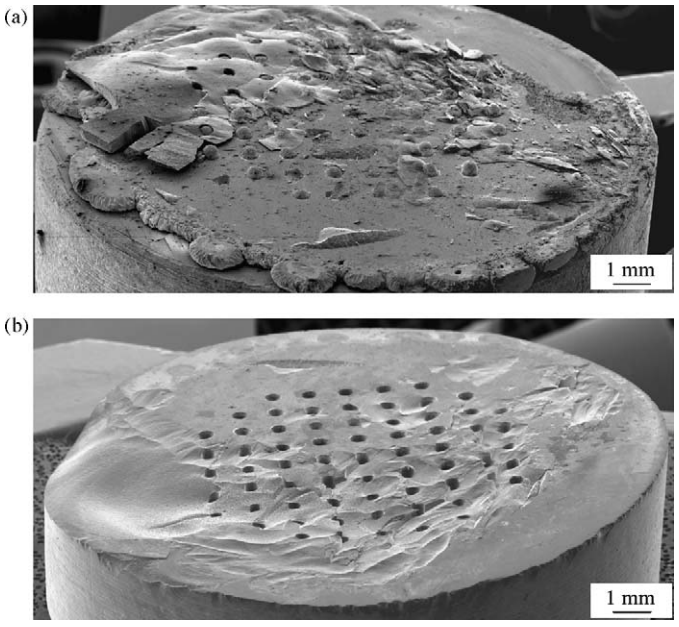

Fig. 12. SEM image (tilt angle $\alpha = 65^{\circ}$) of a characteristic fracture surface of a cone structured ceramic–steel joint: fracture line runs from the ceramic along through the ceramic–braze interface (a) metal part and (b) ceramic part.

about 400 μm. This fractional infill has lead to a better bonding between ceramic and braze metal. The fracture surfaces presented different aspects: the compound failed in parts at the interface ceramic–braze, so that remaining peaks of the braze metal were found on the surface of the steel base. In other parts the fracture line proceeded through the ceramic. In some samples a strong bonding inside the cone structures was achieved, so that the braze filler remained in the holes. The Weibull modulus m scaled with the characteristic values of the shear strength. The highest modulus $m = 5.5$ was accomplished by the cone structured pellet joints, and the weakest braze joints with channel structuring exhibited also the lowest Weibull modulus $m = 2.3$.

4. Summary and conclusions

Within the framework of our studies it was shown, that no wetting of SiC by commercial AgCuTi braze fillers could be achieved by the laser brazing process. However, a good wettability with a contact angle less than 30° on SiC could be observed by using SnAgTi-pellets with a Sn content above 30 wt.% as a braze filler in the laser brazing process. The variation of the Sn/Ag fraction resulted in a very good wetting behaviour for all SnAgTi-fillers.

The EDX-analysis gave neither an explicit evidence, why the SnAgTi-fillers exhibited a better wetting on SiC than the AgCuTi-alloy, nor did it prove differences in wetting of the various SnAgTi-fractions.

However, it was found by other authors, that the low surface energy and the low liquidus temperature of Sn were crucial factors for enhanced wetting of active filler alloys on ceramic [1,30]. Nicholas and Standing came to the result, that the solubility of Ti in ternary systems was reduced by the addition of an element with a low surface energy like Sn.

In that manner the activity of Ti, which is necessary for the diffusion process at the ceramic–braze interface, could be increased so that the ceramic–braze interface was strengthened. Moreover the low solidus temperature (200 °C) and the small Youngs modulus of Sn leads to a reduction of residual stresses, which has a positive effect on the compound strength.

However, the analysis of the micrographs exhibited thin and non-continuous reaction layers towards the ceramic. At the same time Ti-rich particles were found in interface distal regions. The large size of the Ti particles with a reduced mobility was presumed to be the reason for the poor reaction zone.

The application of surface patterns and modifications were investigated in order to improve the poor wettability. But the results of this surface treatment did not result in an improvement with respect to wetting and adherence.

The laser brazed joints with plane grinded SiC pellets and SnAgTi braze fillers achieved a characteristic shear strength of $\tau = 19.1$ MPa. Different surface patterns were applied on the ceramic joining faces with the aim of improving the bonding between the ceramic and the braze metal. The mechanical tests showed a strong reduction of the shear strength by the flat (30 μm) structures of crossed channels down to $\tau = 5.2$ MPa. Whereas a deeper cone shaped structuring provoked an increase of shear strength to a value of $\tau = 24.5$ MPa. The cones were partially filled with braze metal, so that an additive mechanical anchoring was achieved. The fracture surfaces were predominantly found along the ceramic–braze interface. The origin of the fracture was traced back to the thin and irregular produced reaction layer, which was visible for the structured and the non-structured compounds.

Acknowledgements

The author wishes to thank M. Beiser for the preparation of the laser textured ceramic samples as well as F. Lutz for manufacturing the braze pellets. These studies were supported by the Deutsche Forschungsgemeinschaft (DFG) in context with the Sonderforschungsbereich 483 ‘‘High performance sliding and friction systems based on advanced ceramics’’.

References

[1] M.G. Nicholas, T.M. Valentine, M.J. Waite, The wetting of alumina by Cu alloyed with Ti and other elements, Journal of Materials Science 15 (1980) 2197–2206.
[2] S. Morozumi, M. Endo, M. Kikuchi, Bonding mechanism between silicon carbide and thin foils of reactive metals, Journal of Materials Science 20 (1985) 3976–3982.
[3] A.J. Moorhead, H. Keating, Direct brazing of ceramics for advanced heavy-duty diesels, Welding Journal 65/10 (1986) 17–28.
[4] J.K. Boadi, T. Yano, T. Iseki, Brazing of pressureless-sintered SiC using Ag–Cu–Ti alloy, Journal of Materials Science 22 (1987) 2431–2434.
[5] K. Suganuma, Y. Miyamoto, M. Koizumi, Joining of ceramics and metals, Annual Review of Materials Science 18 (1988) 47–73.
[6] O.M. Akselsen, Review: advanced in brazing of ceramics, Journal of Materials Science 27 (1992) 1989–2000.

[7] T. Yano, H. Suematsu, T. Iseki, High-resolution electron microscopy of a SiC/SiC joint brazed by a Ag–Cu–Ti alloy, Journal of Materials Science 23 (1988) 3362–3366.
[8] L. Huijie, F. Jicai, Q. Yiyu, Microstructure of the SiC/TiAl joint brazed with Ag–Cu–Ti filler metal, Journal of Materials Science Letters 19 (2000) 1241–1242.
[9] A. Kar, A.K. Ray, Characterization of Al_2O_3–304 stainless steel braze joint interface, Materials Letters 61 (2007) 2982–2985.
[10] R.M. do Nascimento, A.E. Martinelli, A.J.A. Buschinelli, Recent advances in metal–ceramic brazing, Ceramica 49 (2003) 178–198.
[11] K. Suganuma, T. Okamoto, K. Kamachi, Influence of shape and size on residual stress in ceramic/metal joining, Journal of Materials Science 22 (1987) 2702–2706.
[12] H. Chang, S.-W. Park, S.-C. Choi, T.-W. Kim, Effects of residual stress on fracture strength of Si_3N_4/stainless steel joints with Cu-interlayer, Journal of Materials Engineering and Performance 11 (6) (2002) 640–644.
[13] H. Hao, Y. Wang, Z. Jin, Y. Wang, The effect of interlayer metals on the strength of alumina ceramic and 1Cr18Ni9ti stainless steel bonding, Journal of Materials Science 30 (1995) 4107–4111.
[14] M.R. Locatelli, B.J. Dalgleish, K. Nakashima, A.P. Tomsia, A.M. Glaeser, New approaches to joining ceramics for high-temperature applications, Ceramics International 23 (1997) 313–322.
[15] R.A. Marks, D.R. Chapman, D.T. Danielson, A.M. Glaeser, Joining of alumina via copper/niobium/copper interlayer, Acta Materialia 48 (2000) 4425–4438.
[16] J.-W. Park, P.F. Mendez, T.W. Eagar, Strain energy release in ceramic-to-metal joints by ductile metal interlayer, Scripta Materialica 53 (2005) 857–861.
[17] G.-J. Qiao, H.J. Wang, J.-Q. Gao, Z.-H. Jin, Brazing Al_2O_3 to Kovar alloy with Ni/Ti/Ni interlayer and dramatic increasing of joint strength after thermal cycles, Materials Science Forum 486–487 (2005) 481–484.
[18] G. Blugan, J. Kuebler, V. Bissig, J. Janczak-Rusch, Brazing silicon nitride ceramic composite to steel using SiC-particle-reinforced active brazing alloy, Ceramics International 33 (2007) 1033–1039.
[19] G. Blugan, J. Janczak-Rusch, J. Kuebler, Properties and fractography of Si_3N_4/TiN ceramic joined to steel with active single and double layer braze filler alloy, Acta Materialia 52 (2004) 4579–4588.
[20] N.Y. Taranets, H. Jones, Wettability of AlN with different roughness, porosity and oxidation state by commercial Ag–Cu–Ti brazes, Journal of Materials Science 40 (2005) 2355–2359.
[21] H. Xiong, C. Wan, Z. Zhou, Increasing the Si_3N_4/1.25Cr.–0.5Mo steel joint by using the method of drilling holes by laser in the surface of brazed Si_3N_4, Journal of Materials Science Letters 18 (1999) 1461–1463.
[22] A.A. Shirzadi, Y. Zhu, H.K.D.H. Bhadeshia, Joining ceramics to metals using metallic foams, Materials Science and Engineering A 496 (2008) 501–506.
[23] H. Hongqi, J. Zhihao, W. Xiatian, The influence of brazing conditions on joint strength in Al_2O_3/Al_2O_3 bonding, Journal of Materials Science 29 (1994) 5041–5046.
[24] W. Tillmann, E. Lugscheider, R. Xu, J.E. Indacohea, Kinetic and microstructural aspects of the reaction layer at ceramic/metal braze joints, Journal of Materials Science 31 (445) (1996) 452.
[25] M. Brochu, M.D. Pugh, R.A.L. Drew, Joining silicon nitride ceramic using a composite powder as active brazing alloy, Materials Science and Engineering A 374 (2004) 34–42.
[26] O.C. Paiva, M.A. Barbosa, Brazing parameters determine the degradation and mechanical behaviour of alumina/titanium brazed joints, Journal of Materials Science 35 (2000) 1165–1175.
[27] K. Poser, K.-H. Zum Gahr, J. Schneider, Development of Al_2O_3 based ceramics for dry friction systems, Wear 259 (2005) 529–536.
[28] A. Albers, A. Arslan, M. Mitariu, Clutches using engineering ceramics as friction material, Materialwissenschaften und Werkstofftechnik 36 (3/4) (2005) 102–107.
[29] M. Rohde, I. Südmeyer, A. Urbanek, M. Torge, Joining of alumina and steel by a laser supported brazing process, Ceramics International 35 (2009) 333–337.
[30] Y.H. Chai, W.P. Weng, T.H. Chuang, Relationship between wettability and interfacial reaction for Sn10AgTi on Al_2O_3 and SiC substrates, Ceramics International 24 (1998) 273–279.
[31] R. Standing, M.G. Nicholas, The wetting of alumina and vitreous carbon by copper–tin–titanium alloys, Journal of Materials Science 13 (1978) 1509–1514.
[32] Y. Bao, H. Zhang, Y. Zhou, A simple method for measuring tensile and shear bond strength of ceramic–ceramic and metal–ceramic joining, Materials Innovations 6 (2002) 277–280.
[33] H. Mizuhara, E. Huebel, T. Oyama, High reliability of ceramic to metal, Ceramic Bulletin 68 (9) (1989) 1591–1599.
[34] W. Weibull, A statistical theory of the strength of materials, in: Proceedings of the Ing. Vetenskapakad 151, Stockholm, 1939.